Journal of Zhejiang University-SCIENCE A (Applied Physics & Engineering)
ISSN 1673-565X (Print); ISSN 1862-1775 (Online)
www.zju.edu.cn/jzus; www.springerlink.com
E-mail: kwhlee@berkeley.edu

Improved thermal performance of a hydronic radiant panel heating system by the optimization of tube shapes

Young T. CHAE[1], Kwang Ho LEE[†‡2], Jae Sung PARK[3]

([1]*School of Architecture, University of Illinois at Urbana-Champaign, Urbana, IL 61801, USA*)

([2]*Department of Architectural Engineering, Hanbat National University, Daejeon 305-719, South Korea*)

([3]*Department of Mechanical Engineering, University of Illinois at Urbana-Champaign, Urbana, IL 61801, USA*)

[†]E-mail: kwhlee@hanbat.ac.kr

Received Aug. 1, 2010; Revision accepted Dec. 19, 2010; Crosschecked Mar. 29, 2011

Abstract: The thermal performance enhancement of the hydronic radiant floor heating system by tube shape refinements is investigated in this paper. Both analytical and detailed numerical modelings are carried out to predict the performance of the radiant system. While the simple analytical model briefly investigates the possibility of the effect of the tube shape improvement with the parametric analysis, the commercial computational fluid dynamics (CFD) code (Ansys/CFX) is used to perform the detailed 3D analysis under different tube shape conditions. The fin thickness, the number of fins, and the tube thermal conductivity turn out to have significant effects on the radiant system performance. The potential energy saving impacts of the tube shape refinements are also discussed. The tube shape improvement turns out to increase the floor surface temperature and to decrease the hot water temperature drop across the system, resulting in heating energy savings.

Key words: Radiant panel system, Analytical modeling, Computational fluid dynamics (CFD), Tube shape, Energy saving
doi:10.1631/jzus.A1000358 **Document code:** A **CLC number:** TU83

1 Introduction

Radiant floor heating systems use pipes in which the hot water can be circulated to provide the heating effect on the space. The pipe is embedded into a concrete floor and thus the circulating hot water warms the surrounding concrete structure, which, in turn, directly radiates heat into the space. Radiant floor heating systems have been considered to be more energy efficient than conventional forced air heating systems, since they can provide equal thermal comfort to occupants at lower air temperatures due to higher mean radiant temperatures.

Due to the significant advantage over conventional forced air systems, a variety of research have been performed on radiant floor heating systems. Cho and Zaheer-uddin (1999) conducted an experimental study to comparatively evaluate the performances of two different control schemes for the radiant floor heating system. Those two control schemes are conventional on-off control and two-parameter switching control (TPSC). The TPSC showed a better performance in controlling the indoor temperature (Cho and Zaheer-uddin, 1999). Chen (2002) applied a sophisticated algorithm for generalized predictive control (GPC) to radiant floor heating systems. The GPC was compared with another two control strategies, i.e., on-off and proportional-integral (PI) controls, and was determined to be superior to those two control schemes. Laouadi (2004) developed a detailed semi-analytical model combining 1D numerical software and a 2D analytical model. The model was validated against a full 2D numerical model and showed a good agreement. Bozkir and Canbazoglu (2004) developed an unsteady mathematical model for

‡ Corresponding author

serial and parallel duct floor heating system using hot airflow, and a good agreement was observed between theoretical and experimental data.

However, parametric studies have not been actively performed when compared to experimental studies and computational modeling studies mentioned above. Therefore, it was not easy to find the parametric studies on the radiant systems that can be referred to for the present work. Parametric analysis is an important step to get a better understanding of the interconnection among the elements making up the radiant system. Sattari and Farhanieh (2006) conducted a parametric study, focusing on the effects of pipe diameter, pipe material, pipe number, cover thickness, and cover material. The vertical temperature distribution is considered to be the indicator of the system's thermal performance. However, other significant performance indicators of radiant floor heating systems are not taken into account. Those additional indicators include actual heating energy consumption of the system, floor surface temperature distribution, and the lag time. In addition, effects of the tube shape on the radiant system performance have not been studied so far. Since several tube shapes, such as conventional polyethylene cross link (PEX) type, corrugated type, and fin type are available for radiant systems currently, it is worth considering the effect of tube shapes on the system performance.

The purpose of this study is to investigate the possibility enhancing the radiant system's thermal performance by refining the tube shape. Both the analytical approach and the computational fluid dynamics (CFD) solution are performed separately. The primary purpose of the simple analytical model is to confirm the possibility of the thermal performance improvement by the tube shape refinements before performing the detailed CFD analysis and basic parametric analysis for a better understanding of the tube shape impact as a function of each design parameter. Therefore, there is no connection between the analytical and CFD modeling studies in this paper. The parametric analysis is performed using the analytical solution to study the effects of tube shape-related design parameters on the thermal output of the system. Based on the analytical modeling results, the typical heating floor model is simulated using CFD including both steady state and the transient computation to assess the floor surface temperature distributions, water outlet temperature, lag time, and actual heating supply requirement. These procedures are repeated under different tube shape conditions so that the effect of tube conditions on the system performance can be thoroughly evaluated. A commercial CFD code (Ansys/CFX) is chosen for CFD modeling, and the specific modeling algorithm of the analytical approach is provided.

2 Analytical modeling

Before getting into the CFD modeling, a simple analytical modeling is carried out. The purpose of the analytical solution is to perform the preliminary testing and to investigate the possibility of the thermal performance improvement by the tube shape refinements. In this section, a 1D heat diffusion model is chosen and solved for the parametric study, and several assumptions were made as follows: (1) The convection water flow inside the tube is hydrodynamically and thermally developed. (2) The tube has a uniform cross-sectional area in the axial direction. (3) Surface temperatures of the heating floor and the covering surfaces are uniformly distributed. (4) The heat flux direction is 1D. (5) The thermal resistance between the tube and the panel per tube spacing is negligible (ASHRAE, 2000). (6) The heating floor encompassing the tube is homogeneous and has a constant thermal conductivity. (7) Since indoor thermal conditions are somehow stabilized by the thermal mass of the floors and walls, the radiant system is regarded as quasi-steady. (8) The side and the bottom surfaces of the heating floor are perfectly insulated.

Based on these assumptions, the following 1D algorithm is developed for the preliminary testing of the hydronic radiant heating system.

In this study, the thermal resistance network and the effectiveness-number of transfer units (NTU) methods are used. The important thermal outputs of the radiant heating system performance are the heat transfer rate of the hot water within the tube, the water outlet temperature, and the heat flux radiated from the slab surface into the indoor air. To compute those outputs, the overall heat transfer coefficients should be determined using the following thermal resistance values (ASHRAE, 2000):

$$L_{\text{fin}} = nt_{\text{fin}}, \tag{1}$$

$$R_{\text{t,conv,unfin}} = \frac{1}{h_{\text{water}}\pi D_{\text{inner}}(L_{\text{total}} - L_{\text{fin}})}, \tag{2}$$

$$R_{\text{t,cond,unfin}} = \frac{\ln(D_{\text{outer}} / D_{\text{inner}})}{2\pi k_{\text{t}}(L_{\text{total}} - L_{\text{fin}})}, \tag{3}$$

$$R_{\text{p,unfin}} = \frac{t_{\text{p}} - D_{\text{outer}} / 2}{k_{\text{p}} S_{\text{t}} L_{\text{total}}}, \tag{4}$$

$$R_{\text{c}} = t_{\text{c}} / (k_{\text{c}} S_{\text{t}} L_{\text{total}}), \tag{5}$$

$$R_{\text{air}} = 1/(h_{\text{air}} S_{\text{t}} L_{\text{total}}), \tag{6}$$

where $R_{\text{t,conv,unfin}}$ is the thermal resistance due to convection in the tube inner surface where the fins are not attached (K/W), $R_{\text{t,cond,unfin}}$ is the thermal resistance due to conduction between the tube inner and outer surfaces where fins are not attached (K/W), $R_{\text{p,unfin}}$ is the thermal resistance due to conduction within the heating floor (K/W), R_{c} is the thermal resistance due to the conduction between the floor covering lower and upper surfaces (K/W), and R_{air} is the thermal resistance due to the convection between air and tube. L_{fin} is the total fin length (m), L_{total} is the total length (m), n is the number of fins, and t_{fin} is the fin thickness (m). h_{water} is the convective heat transfer coefficient of the water in the tube inner surface (W/(m^2·K)), and h_{air} is the convective heat transfer coefficient of the air on the panel covering (W/(m^2·K)). D_{inner} and D_{outer} are the tube inner and outer diameters (m), respectively. k_{t} is the tube thermal conductivity (W/(m·K)), and k_{p} and k_{c} are the panel and panel covering thermal conductivities (W/(m·K)), respectively. t_{p} and t_{c} are the panel and panel covering thicknesses (m), respectively; S_{t} is the tube spacing (m). h_{water} is a function of Reynolds number Re and Prandtl number Pr, and can be expressed by Incropera *et al*. (2006):

$$h_{\text{water}} = \frac{(k_{\text{water}} / D_{\text{inner}})(Re - 1000)(f_{\text{w}} / 8)Pr}{1 + 12.7\sqrt{f_{\text{w}} / 8}(Pr^{2/3} - 1)}, \tag{7}$$

$$f_{\text{w}} = (0.79 \ln Re - 1.64)^{-2}, \tag{8}$$

where k_{water} is the water thermal conductivity (W/(m·K)).

Since one of the key interests of this study is to investigate the difference in the radiant system thermal performances with and without fins, two different algorithms were used separately to determine the overall thermal resistance of the heating floor. When there are no fins attached to the tubes (baseline model), the overall thermal resistance R_{total} (K/W) can be computed (ASHRAE, 2000):

$$R_{\text{total}} = R_{\text{t,conv,unfin}} + R_{\text{t,cond,unfin}} + R_{\text{p,unfin}} + R_{\text{c}} + R_{\text{air}}. \tag{9}$$

On the other hand, if there are fins attached to the pipes, two separate thermal resistances should be evaluated with different tube parts where fins are attached and not attached (Kilkis *et al.*, 1995; Incropera *et al.*, 2006):

$$R_{\text{t,conv,fin}} = 1 / (h_{\text{water}}\pi D_{\text{inner}} L_{\text{fin}}), \tag{10}$$

$$R_{\text{t,cond,fin}} = \frac{\ln(D_{\text{outer}} / D_{\text{inner}})}{2\pi k_{\text{t}} L_{\text{fin}}}, \tag{11}$$

$$R_{\text{p,fin}} = \frac{t_{\text{p}} - D_{\text{fin}} / 2}{k_{\text{p}} S_{\text{t}} L_{\text{total}}}, \tag{12}$$

$$R_{\text{fin}} = \frac{\ln(D_{\text{fin}} / D_{\text{outer}})}{2\pi k_{\text{fin}} L_{\text{fin}}}, \tag{13}$$

$$R_{\text{u,fin}} = R_{\text{t,conv,fin}} + R_{\text{t,cond,fin}} + R_{\text{p,fin}} + R_{\text{fin}}, \tag{14}$$

$$R_{\text{u,unfin}} = R_{\text{t,conv,unfin}} + R_{\text{t,cond,unfin}} + R_{\text{p,unfin}}, \tag{15}$$

$$R_{\text{u,tot}} = \frac{1}{1 / R_{\text{u,unfin}} + 1 / R_{\text{u,fin}}}, \tag{16}$$

where $R_{\text{t,conv,fin}}$ is the thermal resistance due to convection between water and fin (K/W), $R_{\text{t,cond,fin}}$ is the thermal resistance due to the conduction between inner and outer tube surfaces (K/W), $R_{\text{p,fin}}$ is the thermal resistance due to the conduction within the heating slab part where the fins are attached to the tubes (K/W), R_{fin} is the thermal rensiance due to the conduction between fin and tube surfaces (K/W), $R_{\text{u,fin}}$ is the total thermal resistance within the heating slab part where fins are attached (K/W), $R_{\text{u,unfin}}$ is the value where fins are not attached (K/W), and $R_{\text{u,tot}}$ is the overall panel thermal resistance (K/W). D_{fin} is the fin outer diameter (m), and k_{fin} is the fin thermal conductivity (W/(m·K)).

As a result, the overall thermal resistance with fins attached to the tubes can be finally calculated as follows (Kilkis *et al.*, 1995; Incropera *et al.*, 2006):

$$R_{\text{total}} = R_{\text{u,tot}} + R_{\text{air}} + R_{\text{c}}. \tag{17}$$

Based on the computed overall thermal resistance, the heat flux through the floor, q_{panel} (W/m^2), the water outlet temperature, $T_{water,out}$ (K), and the radiant system heat transfer rate, Q_{panel} (W), can be finally calculated (Kilkis *et al.*, 1995; Incropera *et al.*, 2006):

$$q_{panel} = (T_{water,in} - T_{air}) / R_{total}, \quad (18)$$

$$T_{water,out} = T_{water,in} - \varepsilon(T_{water,in} - T_{air}), \quad (19)$$

$$\varepsilon = 1 - \exp(-NTU), \quad (20)$$

$$NTU = U_{total} / (m_{water} Cp_{water}), \quad (21)$$

$$U_{total} = 1 / R_{total}, \quad (22)$$

$$Q_{panel} = m_{water} Cp_{water} (T_{water,out} - T_{water,in}), \quad (23)$$

where $T_{water,in}$ is the water temperature (K), T_{air} is the air temperature (K), U_{total} is the overall heat transfer coefficient (W/(m^2·K)), m_{water} is the water mass flow rate (kg/s), and Cp_{water} is the water specific heat (J/(kg·K)).

3 Parametric analysis

Using the analytical model based on the assumptions and equations described above, the thermal performance variations of a radiant system can be investigated with regard to some important design parameters. Since the focus of this study is on the tube shape, the relevant parameters such as the number of fins attached to the tube, fin thickness, and the tube thermal conductivity are taken into account. The key output variables under consideration are the overall thermal resistance, panel thermal resistance, and radiant system heat transfer rate, which directly show how much the system thermal performance is changed. The variations of those output values as a function of each design parameter will be discussed.

Fig. 1 illustrates the construction of the radiant heating floor, and Table 1 summarizes the simulation condition of the parametric study. As shown in Fig. 1, the tube is embedded in the concrete slab and the bottom surface is adiabatic. Water inlet temperature and mass flow rate are set to be 50 °C and 0.028 kg/s, respectively. The total tube length of 15 m, tube outer diameter of 0.02 m, tube thickness of 0.003 m, and concrete thickness of 0.18 m are also chosen.

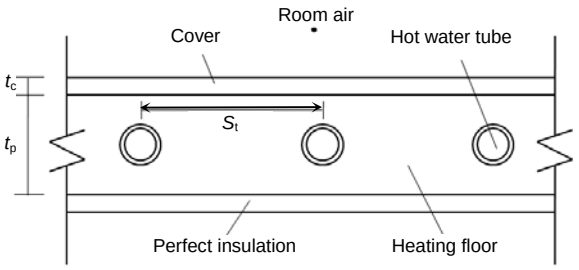

Fig. 1 Radiant heating panel construction
t_p and t_c: panel and panel covering thicknesses, respectively; S_t: tube spacing

Table 1 Simulation conditions

Parameter	Value
Construction	
Total tube length (m)	15
Tube spacing (m)	0.3
Tube outer diameter (m)	0.02
Tube thickness (m)	0.003
Covering thickness (m)	0.005
Concrete thickness (m)	0.18
Thermal property	
Fin thermal cond. (W/(m·K))	400
Concrete thermal cond. (W/(m·K))	1.2
Covering thermal cond. (W/(m·K))	0.16
Convective Co. of air (W/(m^2·K))	9.26
System operation	
Water inlet temperature (°C)	50
Water mass flow rate (kg/s)	0.028
Indoor air temperature (°C)	21
Variable	
Fin thickness (m)	0.001, 0.003, 0.005, 0.008, 0.010, 0.020
Number of fins	0, 20, 40, 60, 80, 100
Tube thermal cond. (W/(m·K))	0.1, 0.3, 0.45, 0.6, 0.8, 1.0

cond.: conductivity; Co.: coefficient

The effects of three design input parameters are evaluated, i.e., the fin thickness, the number of fins, and the tube thermal conductivity. The analysis is performed on six different values of each parameter. The base case values of each variable were set at: 60 for the number of fins, 0.005 m for the fin thickness, and 0.45 W/(m·K) for the tube thermal conductivity (PEX tube). When changing only one variable at every simulation process for parametric studies, the other variables were kept at the baseline values. Note that the heat transfer rate, calculated by the analytical

model, can underestimate the impact of the attached fins due to the fact that it is not a 3D model.

The fin number and the fin thickness would produce the same effect in the analytical model if the total fin length, L_{fin}, is assumed the same. However, those two design parameters should be separately considered in practice, since the surface areas of the fins exposed to the concrete slab are different between each other.

3.1 Effect of fin thickness

The effect of fin thickness on the thermal resistance and the system heat transfer rate is illustrated in Fig. 2. As the fin thickness increases from 0.001 to 0.02 m, the floor panel thermal resistance $R_{u,tot}$ is reduced from 0.032 to 0.023 K/W, and the overall thermal resistance of the entire heating floor R_{total} is reduced from 0.063 to 0.054 K/W with the decreasing rate of 16%. As the fin thickness increases, the total fin length also increases, and thus both $R_{t,conv,fin}$ and $R_{t,cond,fin}$ decrease, while $R_{t,conv,unfin}$ and $R_{t,cond,unfin}$ increase, eventually reducing the overall slab thermal resistance.

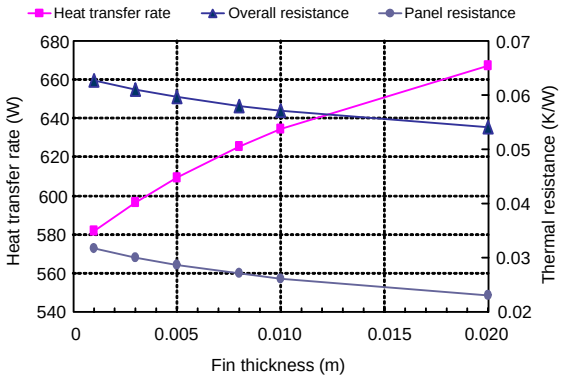

Fig. 2 Effect of fin thickness on the thermal resistance and the system heat transfer rate

Since both R_c and R_{air} remain constant regardless of different fin thicknesses, the difference between $R_{u,tot}$ and R_{total} remains constant and thus those two profiles are parallel to each other as shown in Fig. 2. Due to the reduced thermal resistance, the system heat transfer rate is enhanced from 573 to 627 W, indicating that a larger fin thickness is necessary for the improvement of the radiant system performance. However, the initial and the maintenance costs should also be considered when installing the fins.

3.2 Effect of fin number

The effect of the number of fins attached to the tube on the thermal performance is shown in Fig. 3. As the number of fins rises from 0 to 100, the overall thermal resistance dereases from 0.064 to 0.058 K/W. This is due to the fact that the higher fin number increases the total length of the fin (L_{fin}), and thus the total thermal resistance of the fin part ($R_{u,fin}$) decreases in Eq. (14).

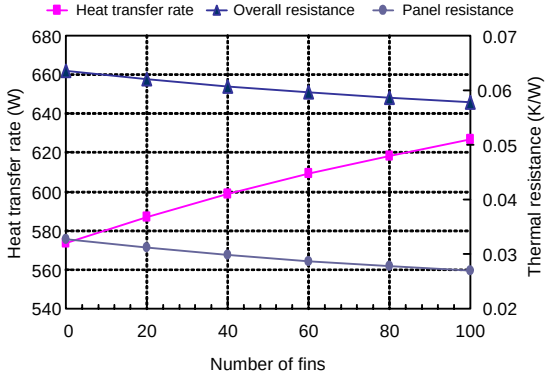

Fig. 3 Effect of the number of fins attached to the tube on the thermal performance

Similar to the fin thickness discussed above, the two different thermal resistance profiles in Fig. 3 are parallel to each other due to the constant R_c and R_{air} regardless of different fin numbers. As a result of the reduced thermal resistance, the system heat transfer rate is enhanced as shown in Fig. 3, indicating that a larger number of fins is also advantageous for the improvement of the radiant system performance. However, other factors such as the costs should also be taken into account for the proper fin design.

3.3 Effect of tube thermal conductivity

The effect of the tube thermal conductivity is illustrated in Fig. 4. As the tube thermal conductivity is improved from 0.1 to 1.0 W/(m·K), the overall thermal resistance decreases from 0.070 to 0.057 K/W with the decreasing rate of 22.5%. As the tube thermal conductivity increases, both $R_{t,cond,fin}$ and $R_{t,cond,unfin}$ decrease, which in turn reduces the overall thermal resistance.

Again due to the constants R_c and R_{air}, the two thermal resistance profiles are parallel to each other. Similarly, the reduced thermal resistance in the heating slab enhances the system heat transfer rate

with the increasing rate of 21%, indicating that the higher tube thermal conductivity is desirable for the better thermal performance. And also at some tube thermal conductivity the improvements begin to level off (Fig. 4).

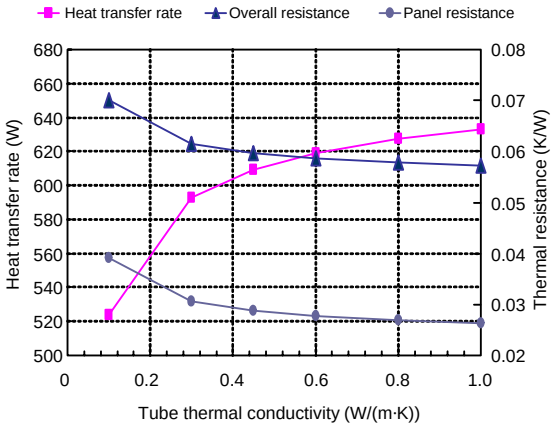

Fig. 4 Effect of tube thermal conductivity

The development of the simple analytical model and the parametric study using the model are discussed. It can be confirmed that the tube shape refinements by the fins does improve the thermal performance of the radiant panel. However, the limitaton of this simple analytical model is that it does not have the capability to consider the multi-dimensional heat flux and the resultant thermal performance changes. Taking this limitation into account, the next part of this study is to carry out the CFD analysis to account for the detailed 3D effect, surface temperature variation, actual heating energy supply, and the time-dependent profiles.

4 Computational fluid dynamics results and discussion

Separated from the simple analytical model discussed above, a commercial CFD software package (Ansys/CFX) is chosen in this study to solve the detailed heat, mass, momentum, and energy balances using the numerical solutions. Both steady-state and transient modeling are carried out. This code is based on a finite-volume method and resolves the Reynolds averaged Navier-Stokes equations for each control volume. The standard *k*-epsilon model is used for turbulence model of the water domain.

The steady-state and transient CFD model is briefly validated by Ahn *et al.* (2006), since the room's geometrical condition and load are quite similar to those of the model of this study. In addition, Ahn *et al.* (2006)'s study is based on the most typical operating conditions of radiant floor heating systems in Korea where radiant heating systems are prevalent in residential buildings. The experimental data of radiant panel heating system for residential buildings in Korea during a specific winter day show a temperature drop of 8 °C from supply temperature (50 °C) to return water temperature (42 °C) under a water mass flow of 2 L/min, when the mean air temperature of the space was set to the design condition (22 °C). It took almost 3 h to reach the design condition, and the average floor covering temperature (3 mm hardwood covered radiant panel) was 26 °C. Under the same load condition and water mass flow rate, the tube system of this study produces the similar temperature drop (8.46 °C), and the average surface temperature (30 °C) of radiant panel. Two datasets are in good agreement, and thus the CFD model would properly predict the radiant heating panel performance, even though there is a small discrepancy due to different weather conditions.

4.1 Steady-state condition

The simulation conditions of CFD analysis are summarized in Table 2. To determine the heating load that should be taken by the radiant floor, indoor and outdoor temperatures of 23 and −17.3 °C, the wall and window *U*-values of 0.5 and 2.0 W/K, and the infiltration of 1.0 air change rate (ACH) were assumed, resulting in the total heating load of 902.6 W, which is kept constant throughout this study. The temperature difference between the indoor temperature setpoint and the outdoor air temperature is taken into account along with the infiltration rate of 1.0 ACH to calculate the heating load caused by the infiltration. Fig. 5 illustrates the room overview, which is composed of two exterior and two interior walls, a roof, a window, and a radiant heating panel.

Three different cases were simulated: the base case with PEX tube (Case A), corrugated tube (Case B), and copper fins attached to Case A (Case C). Since it is extremely complicated to directly model the geometry of corrugated tube, the tube diameter of 0.022 m is specified whose surface area is equivalent

Table 2 Simulation conditions of CFD analysis

Parameter	Value
Construction	
Total tube length (m)	28
Tube spacing (m)	0.3
Tube outer diameter (m)	0.015
Slab thickness (m)	0.06
Fin outer diameter (m)	0.03
Fin thickness (m)	0.003
Thermal property	
Fin thermal conductivity (W/(m·K))	400
Concrete thermal conductivity (W/(m·K))	2.0
System operation	
Water inlet temperature (°C)	45
Water mass flow rate (kg/s)	0.025
Indoor air temperature (°C)	23
Outdoor air temperature (°C)	–17.3
Room boundary condition	
Exterior wall *U*-value (W/K)	0.5
Fenestration *U*-value (W/K)	2.0
Interior wall	Adiabatic
Ceiling	Adiabatic
Infiltration/air change rate	1.0

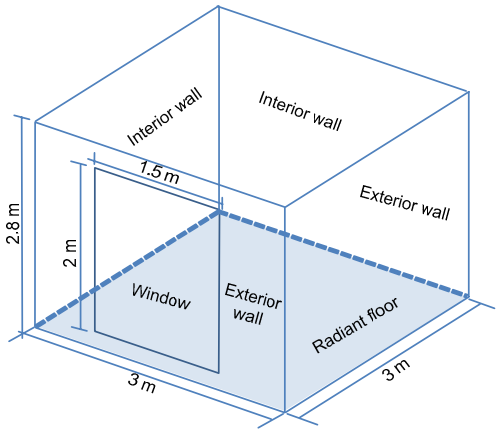

Fig. 5 Room dimension

to 1.5 times that of Case A. In Case C, 100 copper fins with the diamater of 0.03 m are attached to the PEX tube. Figs. 6 and 7 show the tube and fin configurations. The total number of elements in Case C reaches 3279012. Note that the room air is not modeled in this study. Only the slab model is simulated, since the primary purpose of this study is to investigate the slab thermal performance under different tube shape conditions. In other words, approximately 900 W of the heating load is induced into the slab, and the slab is modeled to meet the given heating load. Therefore, the pure effect of different tube shapes on the slab thermal behavior under the same heating load conditions can be investigated.

The steady-state simulation is conducted to determine the floor surface temperature required to meet the heating load of 900 W. Based on the required floor temperature determined in the steady-sate simulation, the transient simulation is performed to investigate the heating supply required to maintain that floor

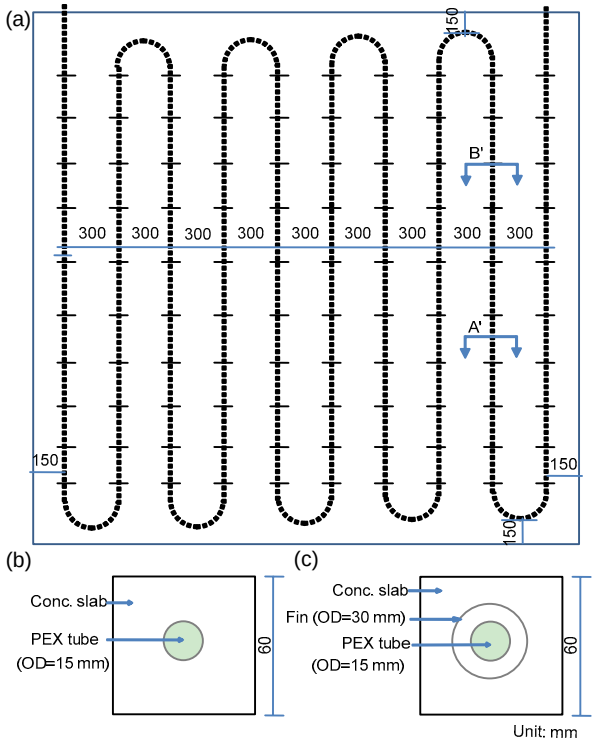

Fig. 6 Tube configuration

(a) Plan view of the slab model; (b) Section view of A′; (c) Section view of B′. OD: outer tube diameter; Conc.: concrete

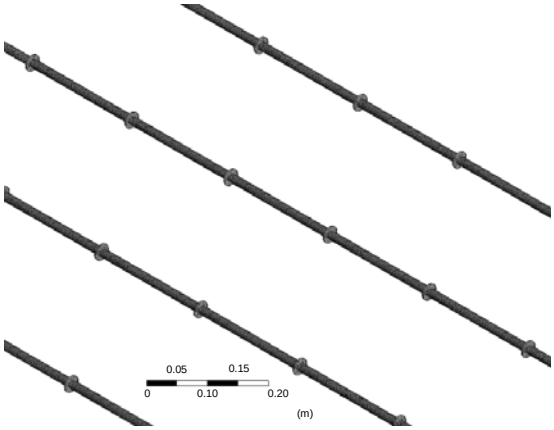

Fig. 7 Tube/fin detail

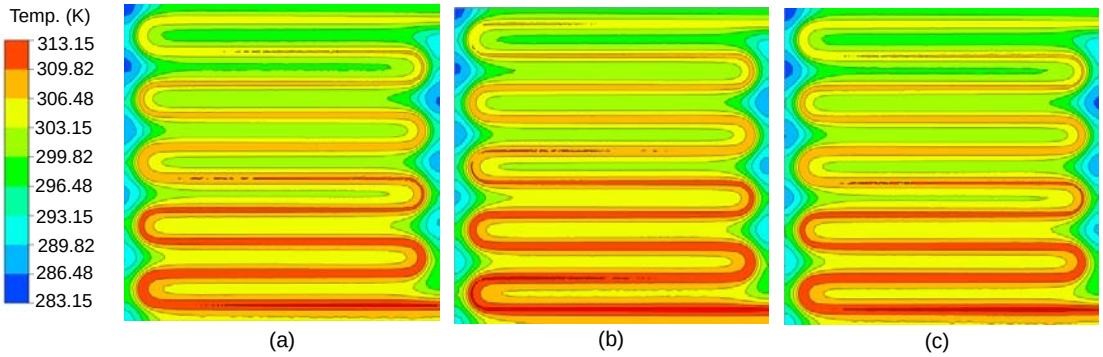

Fig. 8 Surface temperature distribution (steady-state simulation)
(a) Case A; (b) Case B; (c) Case C

surface temperature. From the steady-state simulation, it turns out that the required average floor surface temperature to meet the heating load of 900 W should be around 30 °C for all the three cases. More specifically, Cases A and C require 30.7 °C, and Case B requires 31.3 °C. Those heating floor surface temperature distributions are illustrated in Figs. 8 and 9. The difference in the required floor surface temperatures to meet the given thermal load among different cases indicates that the thermal transmittance performance can be enhanced with the tube shape improvement under the same amount of hot water supply. Due to the nature of the steady-state simulation, the required heating supply for the three cases should be the same as 900 W which is the heating load induced into the slab. In summary, the purpose of the steady-state simulation is to determine the floor surface temperature required to meet the heating load of 900 W for the boundary condition of transient simulation, and it turns out that the floor temperature of approximately 30 °C is needed. The next step is to perform the transient simulation to take into account the time lag due to the thermal mass and to look into the time-dependent water temperature, panel temperature, and required heating supply.

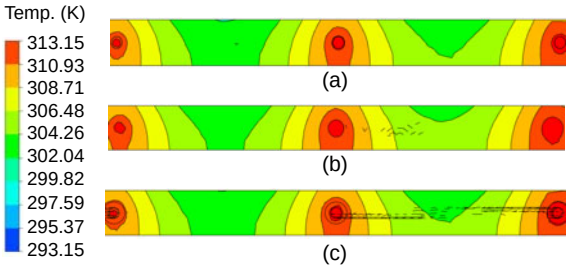

Fig. 9 Vertical temperature distribution (steady-state simulation)
(a) Case A; (b) Case B; (c) Case C

4.2 Transient condition

From the steady-state analysis results, the average floor surface temperature of 30 ºC should be obtained to meet the heating load of 900 W. Since one of the distinct features of the radiant system is the time lag to reach the thermal comfort condition, the transient simulation should be conducted. The pupose of the transient analysis is to investigate how much time and time-dependent heating supply are needed to reach the target floor surface temperature of 30 °C.

The time-dependent variation of the average floor surface temperatures and return water temperatures are illustrated in Fig. 10, and the vertical temperature distribution is presented in Fig. 11, which is the section cut at the center of the slab construction. An important implication of the thermal performance changes due to the tube shape refinement is to look into the difference in the water temperature drop in each case. The less the water temperature drop, the less the heating supply is required to satisfy the given heating load of 900 W. The heating supply is simply a

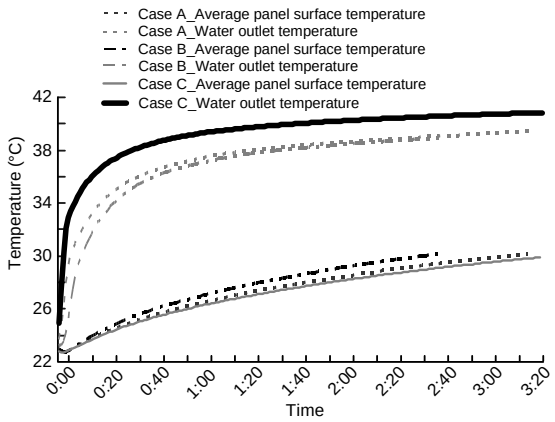

Fig. 10 Time-dependent variations of outlet water and surface temperatures

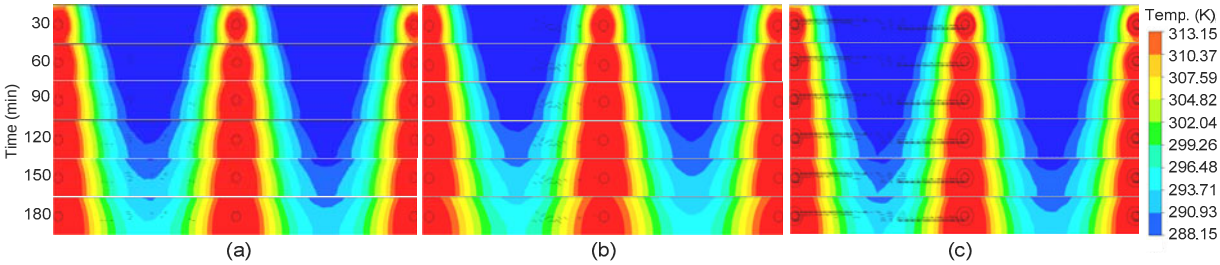

Fig. 11 Transient vertical temperature variation
(a) Case A; (b) Case B; (c) Case C

product of the water specific heat, water mass flow, and outlet and inlet water temperature differences, which indirectly shows the heating energy requirement. As shown in Fig. 10, the water outlet temperature of Case B is the lowest, which means that it has the highest water temperature drop. However, the total heating supply of Case B to get to the 30 ºC surface temperature is lower than that of Case A because much less time is needed to reach the target surface temperature.

On the other hand, in Case C where the copper fins are attached to the water tube, the time to reach the target surface temperature is slightly longer than Case A. However, the return water temperature is always higher than that of the base case, with 23% of the total heating supply being reduced compared to that of Case A. Table 3 summarizes the total heating supply needed to reach 30 °C floor surface temperature.

Table 3 Total heating supply (transient)

Case	Heating supply (kW·h)
Case A	5564
Case B	5050
Case C	4313

From the CFD analysis, it turned out that the total heating supply required to get to the 30 ºC target floor surface temperature was the lowest and that the heating supply to maintain the heat balance condition was also the lowest in Case C. This indicates that under the constant heating load, the significant amounts of heating energy savings can be achieved by properly installing fins.

In Case B where the corrugated tubes are used, once the surface temperature reaches 30 ºC, almost the same amount of heating supply is required as the base case to hold the heating load, but the total heating supply needed to reach the 30 ºC surface temperature is lower compared to the base case due to much less time needed under the assumption of the constant heating load condition. Therefore, it can be concluded that both corrugated tube shape and fins can clearly save the heating energy when properly designed.

5 Conclusions

In this paper, the thermal performance enhancement of the hydronic radiant floor heating system by tube shape improvement is evaluated. Both analytical and detailed CFD simulations were carried out. The modeling algorithm for the simple analytical solution is described, and parametric studies were carried out to assess the impact of each tube design parameter. Furthermore, the floor surface temperature distribution, the return hot water temperature, and the actual heating supply requirement of the radiant floor system were also investigated under both steady-state and transient conditions. The following conclusions were drawn.

1. The fin thickness, fin number, and tube thermal conductivity have significant influences on thermal performance enhancement. The higher thermal conductivity with larger amounts of fins attached to the tube results in the increased thermal performance in agreement with the common sense.

2. From the steady-state simulation, it turns out that the required average floor surface temperature to meet the heating load of 900 W should be around 30 ºC for all the three cases. The difference in the required floor surface temperatures to meet the given thermal load indicates that the thermal transmittance performance can be enhanced with the tube shape improvement.

3. The tube shape refinements can significantly reduce the heating energy consumptions in buildings employing the radiant floor system. The total heating supply required to raise the floor temperature to the target of 30 ºC is the lowest and the heating supply required to maintain the heat balance condition is also the lowest in Case C where fins are attached. In Case B where the corrugated tubes are used, once the surface temperature reaches 30 ºC, almost the same amount of heating supply as the base case is required to hold the heating load, but the total heating supply needed to reach the 30 ºC surface temperature is lower compared to the base case due to much less time needed under the assumption of the constant heating load condition.

Based on this study, the future work includes the actual energy simulation coupled with CFD modeling under the dynamic heating load conditions using the existing energy simulation tools such as EnergyPlus. Another possible improvement is the environmental and economic assessment of the improved tube shape.

References

Ahn, B.C., Sone, J.Y., Lee, T.W., Kim, Y.K., 2006. Simulation and Experimental Study for Energy Flow Dynamics for Floor Radiant Heating System. Proceedings of the Society of Air-Conditioning and Refrigerating Engineers of Korea (SAREK) Summer Annual Conference, Korea.

ASHRAE, 2000. Handbook of Systems and Equipment. American Society of Heating, Refrigerating and Air-Conditioning Engineers Inc. (ASHRAE), Atlanta, USA.

Bozkir, O., Canbazoglu, S., 2004. Unsteady thermal performance analysis of a room with serial and parallel duct radiant floor heating system using hot airflow. *Energy and Buildings*, **36**(6):579-586. [doi:10.1016/j.enbuild.2004.01.039]

Chen, T.Y., 2002. Application of adaptive predictive control to a floor heating system with a large thermal lag. *Energy and Buildings*, **34**(1):45-51. [doi:10.1016/S0378-7788(01)00076-7]

Cho, S.H., Zaheer-Uddin, M., 1999. An experimental study of multiple parameter switching control for radiant floor heating systems. *Energy*, **24**(5):433-444. [doi:10.1016/S0360-5442(98)00101-7]

Incropera, F.P., Dewitt, D.P., Bergman, T.L., Lavine, A.S., 2006. Fundamental of Heat and Mass Transfer (6th Ed.). John Wiley & Sons Inc., Hoboken, USA.

Kilkis, B., Eltez, M., Sager, S., 1995. A simplified model for the design of radiant in-slab heating panels. *ASHRAE Transactions*, **99**(2):210-216.

Laouadi, A., 2004. Development of a radiant heating and cooling model for building energy simulation software. *Building and Environment*, **39**(4):421-431. [doi:10.1016/j.buildenv.2003.09.016]

Sattari, S., Farhanieh, B., 2006. A parametric study on radiant floor heating system performance. *Renewable Energy*, **31**(10):1617-1626. [doi:10.1016/j.renene.2005.09.009]